

Exposure and characterization of nano-structured hole arrays in tapered photonic crystal fibers using a combined FIB/SEM technique

B. C. Gibson, S. T. Huntington, S. Rubanov, P. Olivero

*NANO-MRNF, School of Physics, University of Melbourne,
Parkville, Victoria, Australia, 3010
b.gibson@unimelb.edu.au*

K. Digweed-Lyytikäinen, J. Canning

*Optical Fibre Technology Centre, Australian Photonics Cooperative Research Centre,
University of Sydney, New South Wales, Australia, 2006*

J. D. Love

*Applied Photonics Group, RSPSE, Australian National University,
Canberra, Australian Capital Territory, Australia, 0200*

Abstract: This paper presents a technique to expose and characterize nano-structured hole arrays in tapered photonic crystal fibers. Hole array structures are examined with taper outer diameters ranging from 12.9 μm to 1.6 μm . A combined focused ion beam milling and scanning electron microscope system was used to expose and characterize the arrayed air-silica structures. Results from this combined technique are presented which resolve hole-to-hole pitch sizes and hole diameters in the order of 120 nm and 60 nm, respectively.

© 2005 Optical Society of America

OCIS codes: (060.2310) Fiber optics; (140.3470) Lasers, carbon dioxide; (060.2270) Fiber characterization; (060.2350) Fiber optics imaging; (180.5810) Scanning microscopy.

References and links

1. S. T. Huntington, J. Katsifolis, B. C. Gibson, J. Canning, K. Lyytikäinen, J. Zagari, L. W. Cahill, and J. D. Love, "Retaining and characterising nano-structure within tapered air-silica structured optical fibers," *Opt. Express* **11**, 98–104 (2003), <http://www.opticsexpress.org/abstract.cfm?URI=OPEX-11-2-98>.
2. E. C. Magi, P. Steinvurzel and B. J. Eggleton, "Tapered photonic crystal fibers," *Opt. Express* **12**, 776–784 (2004), <http://www.opticsexpress.org/abstract.cfm?URI=OPEX-12-5-776>.
3. Youngchun Youk, Dug Young Kim and Kun Wook Park, "Guiding properties of a tapered photonic crystal fiber compared with those of a tapered single-mode fiber," *Fiber Integrated Opt.* **23**, 439–446 (2004).
4. Y. K. Lizé, E. C. Mägi, V. G. Ta'eed, J. A. Bolger, P. Steinvurzel and B. J. Eggleton, "Microstructured optical fiber photonic wires with subwavelength core diameter," *Opt. Express* **12**, 3209–3217 (2004), <http://www.opticsexpress.org/abstract.cfm?URI=OPEX-12-14-3209>.
5. C. Kerbage and B. J. Eggleton, "Tunable microfluidic optical fiber gratings," *Appl. Phys. Lett.* **82**, 1338–1340 (2003).
6. S. G. Leon-Saval, T. A. Birks, W. J. Wadsworth, P. St. J. Russell and M. W. Mason, "Supercontinuum generation in submicron fibre waveguides," *Opt. Express* **12**, 2864–2869 (2004), <http://www.opticsexpress.org/abstract.cfm?URI=OPEX-12-13-2864>.
7. B. H. Lee, J. B. Eom, J. Kim, D. S. Moon, U. C. Paek and G. H. Yang, "Photonic crystal fiber coupler," *Opt. Lett.* **27**, 812–814 (2002).

8. T. A. Birks, G. Kakarantzas, P. St. J. Russell and D. F. Murphy, "Photonic crystal fiber devices," in *Fiber-based Component Fabrication, Testing, and Connectorization*, Proc. SPIE **4943**, 142–151 (2002).
9. T. M. Monro, D. J. Richardson, N. G. R. Broderick and P. J. Bennett, "Holey optical fibers: efficient modal model," *J. Lightwave Tech.* **17**, 1093–1102 (1999).
10. J. K. Ranka, R. S. Windeler and A. J. Stentz, "Visible continuum generation in air-silica microstructure optical fibers with anomalous dispersion at 800nm," *Opt. Lett.* **25**, 25–27 (2000).
11. J. C. Knight, J. Broeng, T. A. Birks and P. St. J. Russell, "Photonic band gap guidance in optical fibers," *Science* **282**, 1476–1478 (1998).
12. J. C. Knight, T. A. Birks, P. St. J. Russell and J. P. de Sandro, "Properties of photonic crystal fiber and the effective index model," *J. Opt. Soc. Am. A* **15**, 748–752 (1998).
13. G. A. Valaskovic, M. Holton and G. H. Morrison, "Parameter control, characterization, and optimization in the fabrication of optical fiber near-field probes," *Appl. Opt.* **34**, 1215–28, (1995).
14. R. L. Williamson and M. J. Miles, "Melt-drawn scanning near-field optical microscopy probe profiles," *J. Appl. Phys.* **80**, 4804–4812, (1996).
15. S. Choudhuri, "Microarrays in biology and medicine," *J. Biochem. Molecular Toxicology* **18**, 171–179 (2004).
16. S. T. Huntington, K. Lyytikainen, and J. Canning, "Analysis and removal of fracture damage during and subsequent to holey fiber cleaving," *Opt. Express* **11**, 535–540 (2003), <http://www.opticsexpress.org/abstract.cfm?URI=OPEX-11-6-535>.
17. J. Orloff, M. Utlaut and L. W. Swanson, *High resolution focused ion beams* (Kluwer Academic, New York, 2003).
18. V. Hodzic, J. Orloff and C. Davis, "Focused ion beam created periodic structures on tapered optical fibers," *J. Vac. Sci. Technol. B* **21**, 2711–2714 (2003).
19. A. J. Fielding, K. Edinger and C. C. Davis, "Experimental observation of mode evolution in single-mode tapered optical fibers," *J. Lightwave Technol.* **17**, 1649–1656 (1999).
20. P. Olivero, S. Rubanov, P. Reichart, B. C. Gibson, S. T. Huntington, J. Rabeau, A. D. Greentree, J. Salzman, D. Moore, D. N. Jamieson and S. Praver, "Ion beam assisted lift-off technique for three-dimensional micromachining of free standing single-crystal diamond," in press *Adv. Mater.*
21. M. A. Foster and A. L. Gaeta, "Ultra-low threshold supercontinuum generation in sub-wavelength waveguides," *Opt. Express* **12**, 3137–3143 (2004), <http://www.opticsexpress.org/abstract.cfm?URI=OPEX-12-14-3137>.

1. Introduction

The tapering of photonic crystal fibers post manufacture has proved to be of great interest [1]–[4], with applications ranging from microfluidics [5], to supercontinuum generation [6], couplers [7] and low-loss transition to conventional optical fibers [8]. Photonic crystal fibers, which are also known as holey fibers [9] or microstructured fibers [10], are characterized by an array of microscopic air holes, usually periodic in spacing, in the cladding region which exist along their entire length. Light in this type of fibre can either be confined by the stop bands of the photonic bandgap structure [11] or an average-index effect [12]. Light guidance is possible in the absence of a photonic bandgap where the photonic crystal cladding has an average refractive index that is lower than the central core region. Each of these types of fibre can be made from a single material, the most convenient ones being undoped fused silica or polymer.

CO₂ laser-based pulling methods can be used to taper and break optical fibers to tip diameters in the order of 50 nm [13, 14]. However, when used on photonic crystal fibers to taper structures of this size, this tapering technique forms a solid silica tip where the holes have collapsed. In order to utilize these tapers for applications such as microfluidics and biophotonic DNA nano-array stampers [15], a method must be implemented to expose the arrayed hole structure. Mechanical and polishing techniques are available, however there are limitations with each of these methods due to the size and structure of the tapers. Mechanical cleaving of fiber tapers around one micrometer in diameter can be a highly intricate task and can lead to a large fraction of damage on the endface [16]. In addition, the polishing process is a time intensive procedure which can also lead to the filling of the holes with the polishing solution. Another option for sub-micron cleaving of the tapered structures is to employ Focused Ion Beam (FIB) milling [17]. FIB milling has previously been used to create periodic structures on tapered optical

fibres [18], to observe mode evolution in single-mode tapered fibers [19] and to etch optical waveguides into single crystal diamond [20]. The FIB technique is currently the only feasible method which can be used to expose nano-structured hole arrays within a few microns from the end of an enclosed taper tip.

A combined FIB milling and Scanning Electron Microscopy (SEM) technique has been used to expose and characterize the structure of tapered photonic crystal fibres. Taper cleaving is achieved by scanning a focused beam of gallium ions perpendicular to the propagation axis of the fibre. This precise sub-micron transverse cleaving technique is employed to examine the fiber properties, including the evolution of the hole pitch as a function of taper width.

2. Experiment and results

The photonic crystal fiber used in this paper was manufactured at the Optical Fiber Technology Centre (OFTC) at the University of Sydney, Australia. An optical image of the cross section of the fiber can be observed in Fig. 1, which clearly shows some micro-cracking as a result of the mechanical cleaving process. The fiber has an outer diameter (OD) of $100\ \mu\text{m}$, a typical hole diameter (d) of $2.8\ \mu\text{m}$, a typical hole pitch (Λ) of $6.8\ \mu\text{m}$ and an air fraction of 9%.

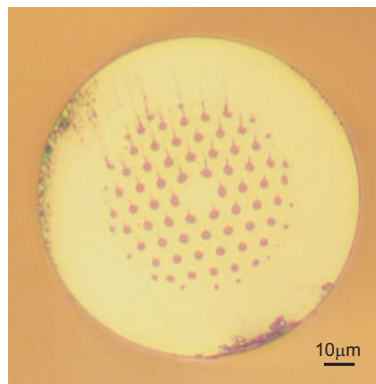


Fig. 1. Optical microscope images of a mechanically cleaved air-silica structured optical fibre with an outer diameter (OD) = $100\ \mu\text{m}$.

The photonic crystal fibre was tapered using a custom-built CO_2 laser-based pulling system. For each sample, a 5 cm length of fiber was stripped of its acrylate coating using methylene chloride and then cleaned with ethanol. The partially stripped fiber was then held under tension between two pulling arms and a CO_2 laser was used to heat the fibre. The motorized arms pulled the fiber in opposite directions until the fiber thinned and finally snapped to form two individual tapered optical fibers with overall taper lengths of approximately 1.25 mm and tip diameters in the order of 50 nm. All of the fiber tapers described in this paper were completed at room temperature and no additional gas was used to pressurize the holes during the tapering. An example of one of the tapered fibers produced using the CO_2 laser-based pulling system can be observed in Fig. 2(a), where the holes at the taper tip have collapsed. The samples were adhered with carbon tape to a 10 mm diameter circular aluminum SEM stub, with the tapered region of each sample extending over the edge of the holder. The untapered portion of the samples were then coated with conductive silver paste to reduce charging in the SEM.

The tapers were then placed in the combined FIB/SEM system, where the tips were positioned perpendicular to the FIB, which was at an angle of 57° with respect to the SEM axis. The FIB cleaving was performed, perpendicular to the longitudinal direction of the taper, using an Orsay Physics Canon 31M plus FIB column mounted on a JEOL 5910 SEM and equipped

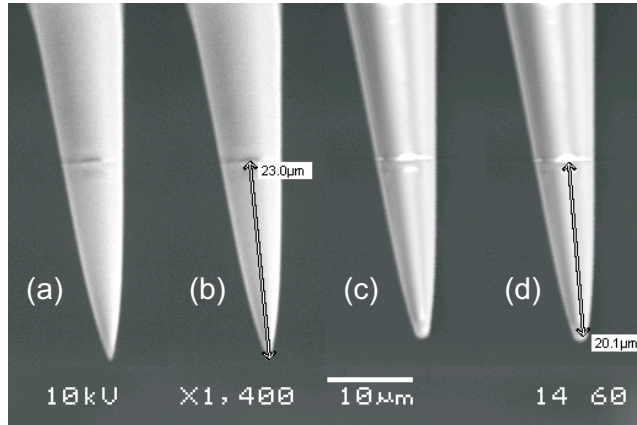


Fig. 2. (a), (b) show SEM micrographs of the tapered fiber prior to FIB cleaving and (c), (d) show the tapered fiber after 2.9 μm of silica has been removed with the FIB in order to expose the hole array.

with a Raith Elphy Quantum ion beam lithography package for the automated machining of user-defined patterns. The FIB provided a 30 keV Ga^+ ion beam with a current of approximately 280 pA and a spot size of around 500 nm. The simultaneous imaging was performed via the SEM.

Figures 2(a) and (b) depict SEM micrographs of a tapered photonic crystal fibre with a reference mark, milled with the FIB, at a distance of 23.0 μm from the tip of the taper. Figures 2(c) and (d) show the same tapered photonic crystal fibre after having been cleaved with the FIB. A video screen grab of the FIB cleaving process is shown in Fig. 3, which depicts the instant before 2.9 μm of the taper tip is removed in order to expose the arrayed hole structure.

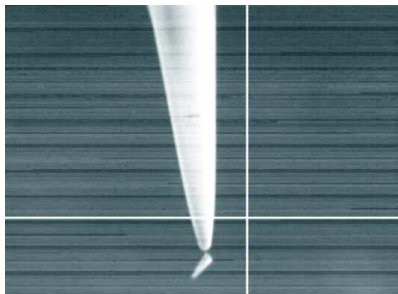


Fig. 3. The video screen grab shows the instant before 2.9 μm of the tip of the taper is totally removed due to the FIB-based cleaving process (AVI, 2,520 kb).

Four examples of the FIB-cleaved fiber ends, with diameters ranging from 12.9 μm to 1.6 μm , can be observed in Fig. 4(a) to (d). Figure 4(a) shows an optical image of a cleaved fiber endface which has been tapered by a factor of $\sim 8:1$ with an OD of 12.9 μm and $\Lambda \sim 890$ nm. In comparison to the untapered fiber shown in Fig. 1, there appears to be no change to the hole array structure. Figure 4(b) shows a SEM micrograph of a portion of the fiber endface which has been tapered by a factor of $\sim 14:1$ (OD of 7.2 μm and $\Lambda \sim 581$ nm). Figures 4(c) and (d) show SEM micrographs of the entire endface of FIB-cleaved photonic crystal fibres which have been tapered by factors of $\sim 29:1$ (OD of 3.5 μm and $\Lambda \sim 246$ nm) and $\sim 63:1$ (OD of 1.6 μm and $\Lambda \sim 120$ nm), respectively. There appears to be a minimal reduction in

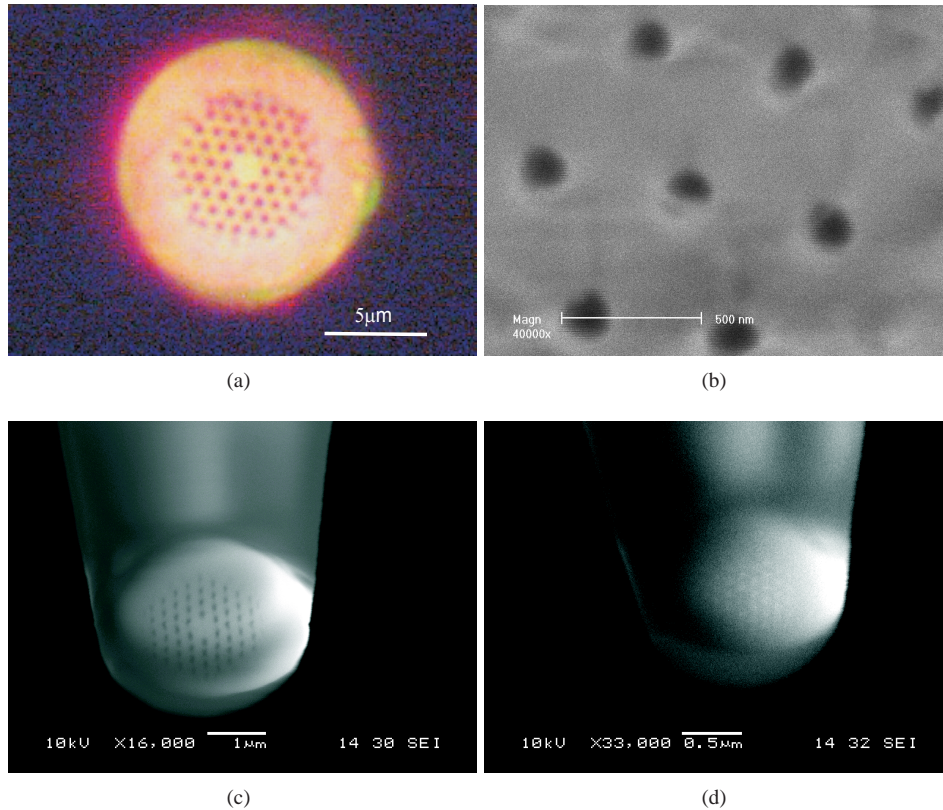


Fig. 4. FIB-cleaved fiber ends: (a) Optical image where the OD = $12.9 \mu\text{m}$, $\Lambda \sim 890 \text{ nm}$ and SEM micrograph images where (b) the OD = $7.2 \mu\text{m}$, $\Lambda \sim 581 \text{ nm}$, (c) the OD = $3.5 \mu\text{m}$, $\Lambda \sim 246 \text{ nm}$ and (d) the OD = $1.6 \mu\text{m}$, $\Lambda \sim 120 \text{ nm}$.

the relative hole size for the taper depicted in Fig. 4(c). This reduction may be further delayed through the use of pressurization techniques during the tapering process. Also, the appearance of the ‘white’ holes in Fig. 4(d) indicate possible sample charging effects during imaging with the SEM. The core sizes in Figs. 4(a), (c) and (d) are shown to scale down linearly with the outer diameter of the taper to $\sim 650 \text{ nm}$, $\sim 180 \text{ nm}$ and $< 100 \text{ nm}$, respectively, which agrees with previously reported findings [21]. The hole pitch, with values ranging from 120 nm , was also found to scale linearly with the outer diameter of the tapered photonic crystal fiber and a plot of this relationship can be observed in Fig. 5. It is expected that Λ will non-linearly approach zero before the taper width reaches $0 \mu\text{m}$. This significant result suggests that true nano-engineering of photonic crystal fibers post manufacture is possible via a judicious choice of tapering parameters.

Photonic crystal fibers, with varying hole sizes and structures, have been previously tapered by factors of $\sim 6:1$ (OD of $30 \mu\text{m}$ and $\Lambda \sim 500 \text{ nm}$) [6], $\sim 6:1$ (OD of $17 \mu\text{m}$ and $\Lambda \sim 170 \text{ nm}$) [2], $\sim 8:1$ (OD of $15 \mu\text{m}$ and $\Lambda \sim 1.1 \mu\text{m}$) [1] and $\sim 50:1$ (OD of $2.7 \mu\text{m}$ and $\Lambda \sim 740 \text{ nm}$) [4], whilst still retaining the original cross-section geometry of the untapered fiber. The results presented in this paper show the first demonstration to our knowledge of a hole-to-hole pitch size of $\Lambda \sim 120 \text{ nm}$ in an array of holes with diameters of $\sim 60 \text{ nm}$ with a core size of $< 100 \text{ nm}$. Nano-arrayed structures with these dimensions have direct applications in the area

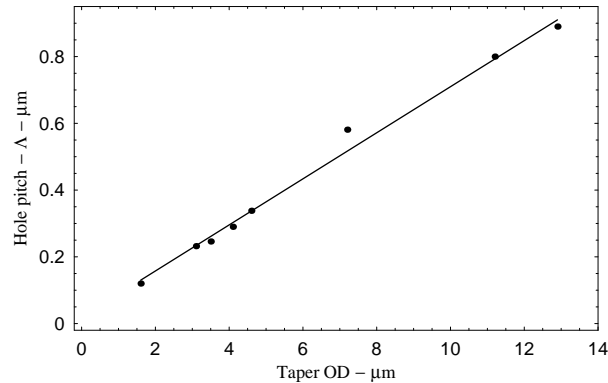


Fig. 5. This plot shows a linear relationship between the hole pitch (Λ) and the outer diameter (OD) of the tapered photonic crystal fibers.

of biophotonic DNA stampers, where there is an immediate need to reduce the size and spacing of the DNA samples in order to greatly increase the number of simultaneous tests. It is possible that even smaller array structures may be retained for taper diameters less than $1.6 \mu\text{m}$.

The clear advantage of the combined FIB/SEM-cleaving technique lies in its use to produce smooth cuts across the entire endface of the taper, which avoids the crack fronts that are typically observed in photonic crystal fibers when mechanical cleaving is performed [16]. The FIB can be used to directly expose the inner hole structure of the tapered fiber and the SEM can be used to directly image the endface of the FIB-cleaved optical fiber. Prior to FIB-cleaving, the tapered fibres appeared to not exhibit any hole structure at the tip. The use of the FIB/SEM technique revealed that the hole array structure is maintained almost to the end of the tapered fiber. This combined cleaving technique may potentially be applied to tapered photonic crystal fibres with sub-micron width dimensions in order to resolve smaller hole arrays.

3. Conclusion

This paper has demonstrated the use of a combined FIB/SEM technique to simultaneously expose and characterize nano-structured hole arrays in tapered photonic crystal fibers. Exposing, or cleaving, of the samples was performed by scanning a focused beam of gallium ions perpendicular to the propagation axis of the fibre and the sample characterization was undertaken with a SEM. Fiber samples were tapered to form two individual tips and then cleaved with outer diameters ranging from $12.9 \mu\text{m}$ to $1.6 \mu\text{m}$. The hole-to-hole spacing was found to vary linearly with the outer diameter of each of the examined tapers. In addition, the use of a combined FIB/SEM cleaving technique has resulted in the first demonstration to our knowledge of $\Lambda \sim 120 \text{ nm}$ in an array of holes with diameters of $\sim 60 \text{ nm}$ with a core size of $< 100 \text{ nm}$. These nano-structured hole arrays have the potential for a range of exciting new applications such as microfluidics and biophotonic DNA stamping devices.

Acknowledgements

This project is proudly supported by the International Science Linkages programme established under the Australian Government's innovation statement Backing Australia's Ability. The Australian Research Council's Center of Excellence - Center for Quantum Computer Technology (CQCT) funded the FIB/SEM infrastructure. An ARC Discovery Project Grant was used to fund fiber fabrication. The authors would also like to acknowledge J. Digweed, J. Zagari and S. Crawford for their assistance with sample preparation and useful discussions.